Mitochondrial Fatty Acid Synthase Utilizes Multiple Acyl Carrier Protein Isoforms[1][OPEN]

Xinyu Fu,[a,b,c] Xin Guan,[a,b,c] Rachel Garlock,[a] and Basil J. Nikolau[a,b,c,2,3]

[a]Roy J. Carver Department of Biochemistry, Biophysics, and Molecular Biology, Iowa State University, Ames, Iowa 50011
[b]Center for Biorenewable Chemicals (CBiRC), Iowa State University, Ames, Iowa 50011
[c]Center for Metabolic Biology, Iowa State University, Ames, Iowa 50011

ORCID IDs: 0000-0003-4178-238X (X.F.); 0000-0002-7983-2103 (X.G.); 0000-0002-4672-7139 (B.J.N.).

Acyl carrier protein (ACP) is a highly conserved cofactor protein that is required by Type II fatty acid synthases (FASs). Here, we demonstrate that up to three mitochondrial ACP (mtACP) isoforms support the Arabidopsis (*Arabidopsis thaliana*) mitochondrially localized Type II FAS. The physiological importance of the three mtACPs was evaluated by characterizing the single, double, and triple mutants. The *mtACP1* (At2g44620), *mtACP2* (At1g65290), and *mtACP3* (At5g47630) single mutants showed no discernible morphological growth phenotype. Functional redundancy among the three mtACPs was indicated by the embryo-lethal phenotype associated with simultaneous loss of all three *mtACP* genes. Characterization of all double mutant combinations revealed that although the *mtacp1 mtacp3* and *mtacp2 mtacp3* double mutant combinations showed no observable growth defect, the *mtacp1 mtacp2* double mutant was viable but displayed delayed growth, reduced levels of posttranslationally lipoylated mitochondrial proteins, hyperaccumulation of photorespiratory Gly, and reduced accumulation of many intermediates in central metabolism. These alterations were partially reversed when the *mtacp1 mtacp2* double mutant plants were grown in a nonphotorespiratory condition (i.e. 1% CO_2 atmosphere) or in the presence of 2% Suc. In summary, mtACP, as a key component of mitochondrial fatty acid biosynthesis, is important in generating the fatty acid precursor of lipoic acid biosynthesis. Thus, the incomplete lipoylation of mitochondrial proteins in *mtacp* mutants, particularly Gly decarboxylase, affects the recovery of photorespiratory carbon, and this appears to be critical during embryogenesis.

At least three enzyme systems, each localized in distinct subcellular compartments, generate fatty acids in plants. The majority of these fatty acids are used as building blocks for cellular lipids (e.g. glycerolipids in membranes and triacylglycerol in seeds). These are primarily produced by a plastid-localized Type II fatty acid synthase (ptFAS), which produces acyl chains of 16–18 carbon atoms (Ohlrogge and Browse, 1995). These fatty acids can be further elongated by the endoplasmic reticulum-localized fatty acid elongase (FAE) system to generate the very-long-chain fatty acids (i.e. acyl chains with >18 carbon atoms), which are primarily used to assemble the epicuticular lipids and sphingolipids (Samuels et al., 2008; Markham et al., 2011). The primary contribution of the mitochondrially localized Type II fatty acid synthase system (mtFAS) appears to be the generation of the fatty acid precursor of lipoic acid, an essential cofactor of several key enzymes in metabolism (Wada et al., 1997; Guan et al., 2015, 2017; Guan and Nikolau, 2016).

Both ptFAS and mtFAS systems utilize acyl carrier protein (ACP) as a cofactor protein that shuttles acyl intermediates between active sites of the catalytic components of each FAS system (White et al., 2005). The ACP-dependent function cannot be accomplished without converting the inactive *apo* form into the active *holo* form via the posttranslational phosphopantetheinylation of a conserved Ser residue (Lambalot et al., 1996). The terminal thiol of the ACP-carried phosphopantetheine arm covalently binds to the acyl intermediates via a high-energy thioester bond (Lambalot et al., 1996).

Prior characterization of the Arabidopsis (*Arabidopsis thaliana*) mtFAS system has identified individual enzymatic components of this system, including phosphopantetheinyl transferase (mtPPT; Guan et al., 2015), malonyl-CoA synthetase (mtMCS; Guan and Nikolau, 2016), β-ketoacyl-ACP synthase (mtKAS; Ewald et al., 2007), and 3-hydroxyacyl-ACP dehydratase (mtHD; Guan et al., 2017), and these studies have established the essential role of mtFAS in plant growth and development. However, the genetic machinery that encodes the mitochondrial ACP component (mtACP) has not been elucidated.

[1]This work was supported by the National Science Foundation (grant no. EEC 0813570) and the U.S. Department of Energy (grant no. 0000217546).

[2]Senior author.

[3]Author for contact: dimmas@iastate.edu.

The author responsible for distribution of materials integral to the findings presented in this article in accordance with the policy described in the Instructions for Authors (www.plantphysiol.org) is: Basil J. Nikolau (dimmas@iastate.edu).

B.J.N., X.F., and X.G. conceived the research plans; X.F. performed the experiments and analyzed the data; R.G. and X.G. provided technical assistance to X.F.; B.J.N. and X.F. wrote the article.

[OPEN]Articles can be viewed without a subscription.

www.plantphysiol.org/cgi/doi/10.1104/pp.19.01468

ACP was initially isolated from plant and bacterial sources in the 1960s (Simoni et al., 1967). Subsequent characterization identified multiple ACP isoforms in plastids (Ohlrogge and Kuo, 1985; Guerra et al., 1986) and mitochondria (Chuman and Brody, 1989; Shintani and Ohlrogge, 1994). In Arabidopsis, eight gene loci can be recognized by sequence homology to encode ACP isoforms, five of which are plastidic ACPs (ptACPs), and three of which appear to be mtACPs (Mekhedov et al., 2000). The plastid isoforms show distinct patterns of expression in response to developmental and environmental cues. Specifically, *ptACP1* (At3g05020), *ptACP2* (At1g54580), and *ptACP3* (At1g54630) are near constitutively expressed in leaves, roots, and seeds (Hloušek-Radojčić et al., 1992), whereas *ptACP4* (At4g25050) is predominantly expressed in leaves and is induced upon illumination of plants (Bonaventure and Ohlrogge, 2002), and *ptACP5* (At5g27200) is preferentially expressed in roots and down-regulated by salt stress (Huang et al., 2017). Mutations in *ptACP4* lead to a chlorotic phenotype with altered fatty acid composition (Branen et al., 2003; Ajjawi et al., 2010).

Here, we characterized the physiological functions of the three putative mtACP-coding genes (At2g44620, At1g65290, and At5g47630) by a reverse genetic strategy. These studies reveal that although mutations in individual *mtACP* genes do not affect growth or development, simultaneous mutations in all three *mtACP* genes is associated with embryo lethality. The analysis of different combinations of *mtACP* double mutants uncovers complex functional redundancies among the three mtACPs, which reveals the dependence of the mtFAS system on mtACP isoforms.

RESULTS

Phylogenetic Analysis of Plant ACP Homologs

Multiple sequence alignment of the Arabidopsis ptACP and mtACP amino acid sequences revealed the common DSLD-motif, which contains the Ser residue that is phosphopantetheinylated to form *holo*-ACPs (Supplemental Fig. S1). The three Arabidopsis mtACP isoforms share between 40% and 54% sequence identity, but considerably lower sequence similarity (33% to 42%) with the five ptACPs. Figure 1 shows the wider phylogenetic context of the Arabidopsis ACPs in relation to ACPs from 39 flowering plants representing major clades of APG IV (The Angiosperm Phylogeny Group, 2016) and three microbial sources (Supplemental Dataset S1). Within the ptACP clade, Arabidopsis ptACP1, ptACP2, ptACP3, and ptACP5 group more closely in a subclade that is separate from the ptACP4 clade, suggesting that the divergence between ptACP4 and the other four ptACPs occurred early in evolution.

The putative mtACP sequences segregate in a separate clade, which is indicative of their distant evolutionary relationship with respect to ptACPs. The mtACP clade includes two previously characterized mtACPs from yeast (*Saccharomyces cerevisiae*; Van Vranken et al., 2016) and *Chlamydomonas reinhardtii* (Blatti et al., 2012). The three Arabidopsis mtACPs fall into three distinct clades, and each of these major clades contains examples of ACPs from both dicot and monocot plants. Hence, we conclude that the emergence of the three mtACP homologs has a deep evolutionary history predating the split between eudicots and monocots.

Experimental Validation of the Mitochondrial Localization of the Putative *mtACP* Gene Products

The in silico predictions of the subcellular localization of the three putative Arabidopsis mtACPs suggest that they are likely to be localized in mitochondria (Supplemental Table S1). Experimental confirmation of these computational predictions was provided by the transgenic expression of each ACP-coding open reading frame (ORF) fused to the ORF encoding the GFP. These transgenes were expressed in planta under the transcriptional control of the 35S promoter, and Figure 2 shows confocal micrographs of the roots of the resulting transgenic plants as compared to control plants. The GFP fluorescence from all three mtACP-fusions colocalized with the mitochondrial marker, MitoTracker. In contrast, no GFP fluorescence signal was detected in the nontransgenic wild-type control plants, and the GFP fluorescence signal from the *p35S::GFP* control plants accumulates in the cytosol. These analyses, therefore, confirm the mitochondrial localization of the mtACP1, mtACP2, and mtACP3 proteins.

Differential Tissue Expression Profiles of *mtACP* Genes

The spatial and temporal expression patterns of the three *mtACP* genes were characterized using RNA extracted from several tissues of wild-type plants. Reverse-transcription quantitative PCR (RT-qPCR) analysis showed that in all tissues examined, the *mtACP1* and *mtACP2* transcripts accumulated at levels 10- to 50-fold higher than those of *mtACP3* (Fig. 3). The lower levels of *mtACP3* mRNA is consistent with the fact that only mtACP1 and mtACP2 proteins have been detected in a prior proteomic study (Meyer et al., 2007). While the expression levels of *mtACP1* and *mtACP3* did not vary among the tissues examined, the expression of *mtACP2* showed an ~3-fold variation among the different tissues examined, with the highest level occurring in flowers and the lowest in young seedling leaves. These expression patterns of *mtACPs* are consistent with public microarray and RNAseq data (Supplemental Fig. S2; Hruz et al., 2008), and are similar to the expression patterns of other characterized mtFAS gene components, such as *mtPPT* (Guan et al., 2015), *mtKAS*, and *mtHD* (Guan et al., 2017).

Characterization of the In Planta Functions of mtACP Isoforms

The physiological roles of the three mtACP isoforms were dissected by characterizing transfer DNA

(T-DNA)-tagged mutant alleles (i.e. *mtacp1*, *mtacp2*, and *mtacp3*). RT-PCR analysis of RNA isolated from plants that are homozygous for the mutant alleles at each locus confirmed that each mutant stock carries null alleles at each locus (Supplemental Fig. S3). Moreover, in each mutant stock, there was no detectable compensatory change in the expression of the other two *mtACP* genes, which are in the wild-type state (Supplemental Fig. S3). Loss of any single *mtACP* isoform (i.e. *mtacp1*, *mtacp2*, and *mtacp3* mutants) did not cause any observable alteration in the morphological appearance or biomass of the resulting plants (Fig. 4; Supplemental Fig. S4), indicating functional redundancy among the three isoforms.

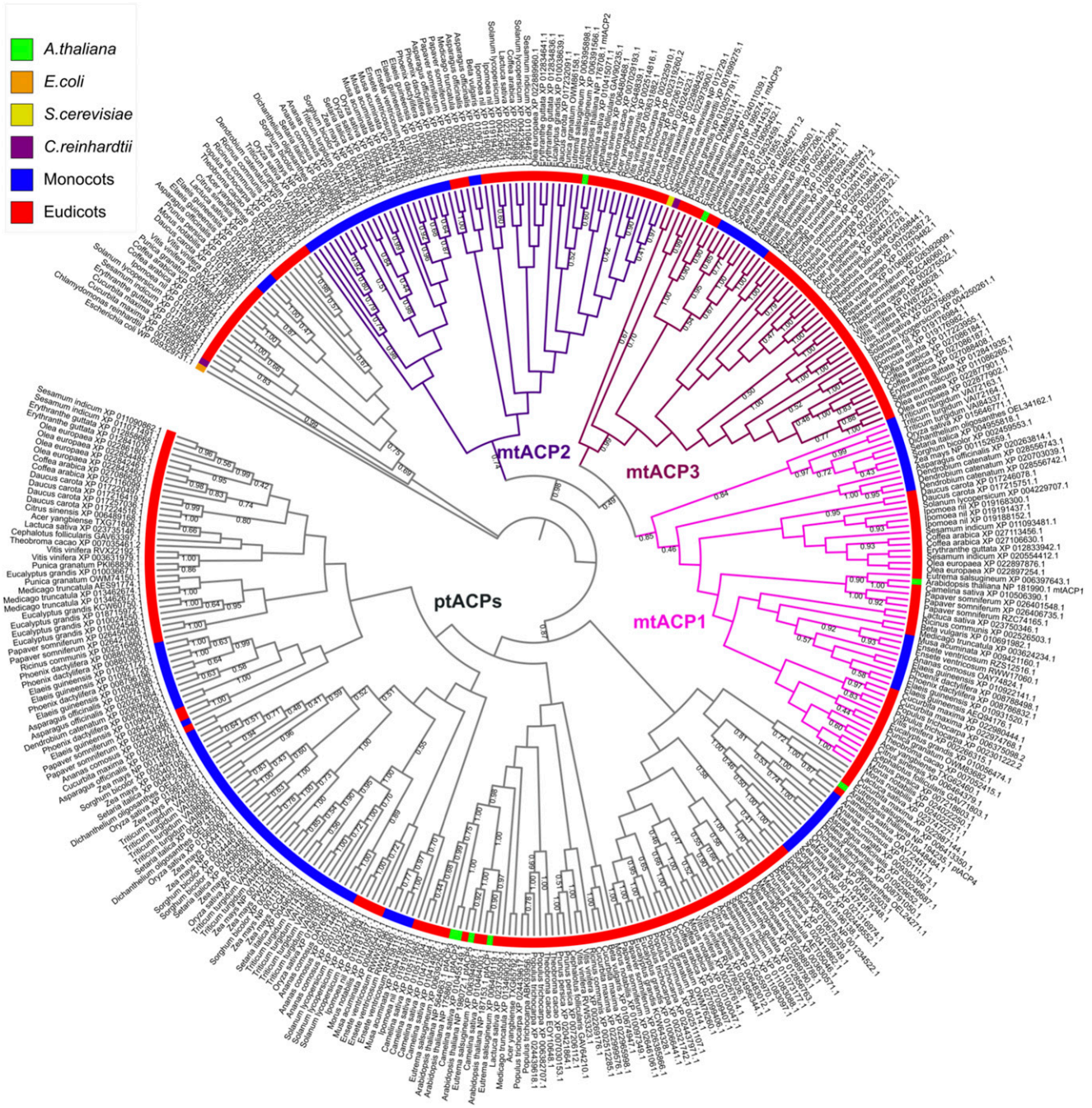

Figure 1. Phylogenetic analysis of ACPs. Plant ACP protein sequences were aligned using the ClustalW program and depicted as a rooted phylogenetic tree using the neighbor-joining method in MEGAX. The protein sequence of *Escherichia coli* ACP was chosen as an outgroup. The numbers at each node represent the bootstrap values using 1,000 replicates. The protein IDs for ACPs are listed in Supplemental Dataset S1.

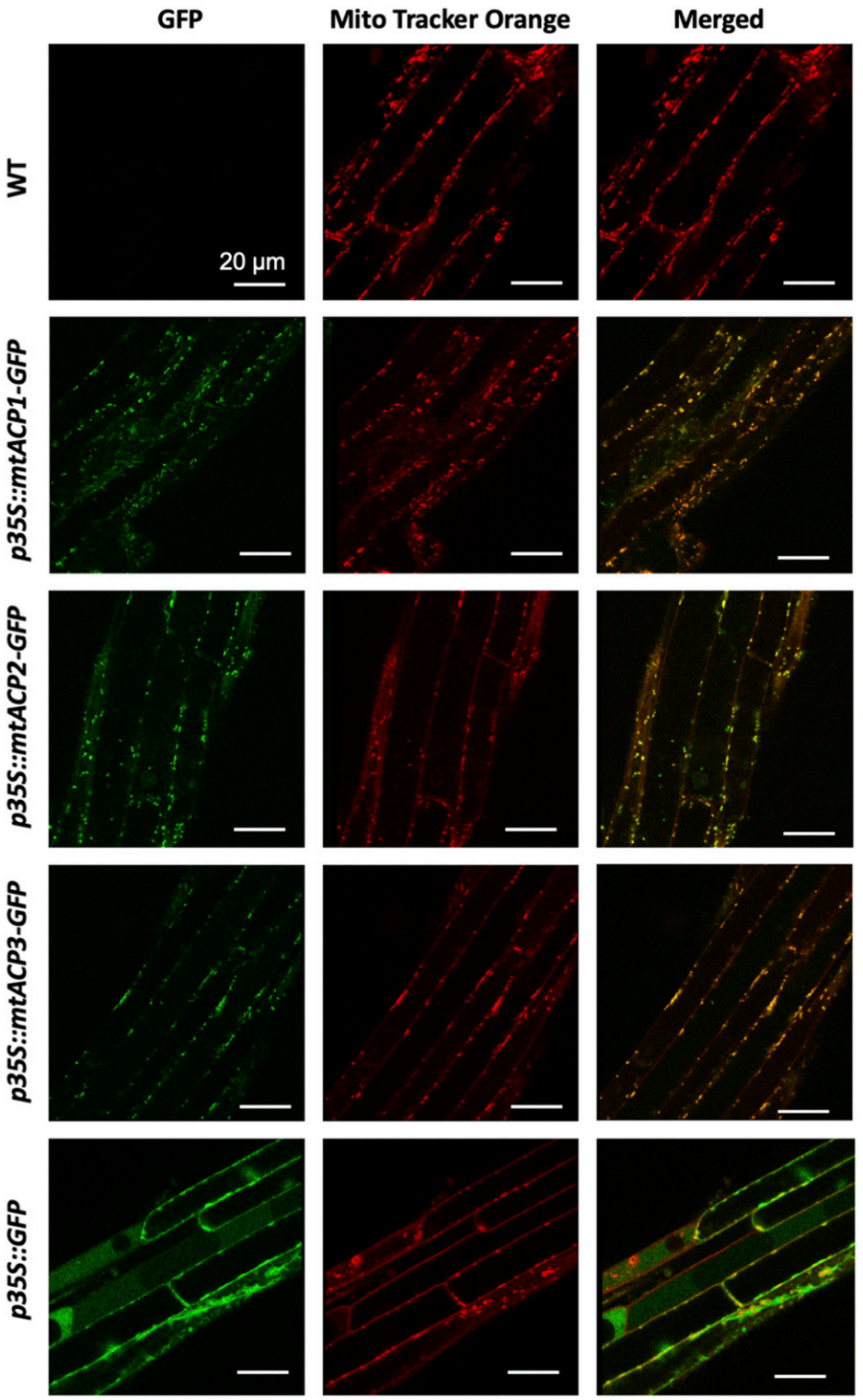

Figure 2. Subcellular localization of Arabidopsis mtACP1, mtACP2, and mtACP3. Each row shows images obtained from wild-type nontransgenic plants or from plants carrying the indicated GFP fusion transgene. Fluorescence signals from roots were monitored by confocal laser scanning microscopy using GFP fluorescence (column 1) and MitoTracker fluorescence (column 2). The resulting images were overlaid (column 3) to indicate the colocalization of GFP with the MitoTracker signal.

The potential genetic redundancy among the mtACP isoforms was explored by characterizing different combinations of homozygous double mutant plants (i.e. *mtacp1 mtacp2*, *mtacp1 mtacp3*, and *mtacp2 mtacp3*). In contrast to the *mtacp1 mtacp3* and *mtacp2 mtacp3* double mutants, which displayed a normal morphological phenotype, the *mtacp1 mtacp2* double mutant exhibited a significant impairment in vegetative and reproductive growth (Fig. 4; Supplemental Fig. S4). Specifically, the *mtacp1 mtacp2* double mutants had only developed two rosette leaves by 16 d after imbibition, whereas by this stage wild-type plants and *mtacp1 mtacp3* and

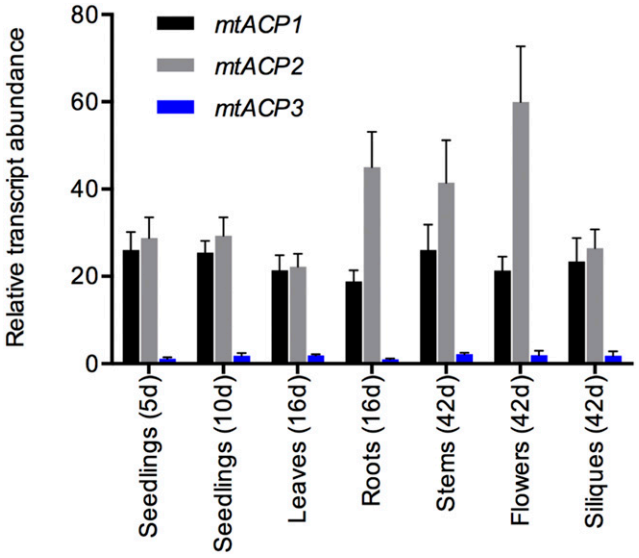

Figure 3. Expression profile of *mtACP* in different Arabidopsis tissues. Data represent the expression level of the individual mtACP isoform mRNA in different tissues of wild-type Arabidopsis plants as quantified by RT-qPCR. The expression levels were normalized against the level of the reference gene, *UQB10*. Values are means ± SE ($n = 5$).

mtacp2 mtacp3 double mutants had developed six rosette leaves. Additionally, the *mtacp1 mtacp2* double mutants had not bolted by 40 d after imbibition, whereas by this time wild-type plants, and *mtacp1 mtacp3* and *mtacp2 mtacp3* double mutants, had bolted and produced siliques. Despite growing more slowly than the wild-type plants, the *mtacp1 mtacp2* double mutants eventually reached full maturity and produced viable seeds.

These morphological delays in the development of the *mtacp1 mtacp2* double mutants are probably associated with the fact that these two genes are expressed at levels 10- to 50-fold higher than *mtACP3*. Hence, in this double mutant there is not sufficient ACP expression in mitochondria to support mtFAS activity. This potential causality was confirmed by overexpression of the *mtACP2-GFP* transgene in this double mutant, which completely restored the growth of the *mtacp1 mtacp2* mutant to wild-type morphology (Supplemental Fig. S5). Furthermore, this indicates that the fusion of the GFP protein sequence does not significantly affect mtACP2 function. This is probably because the two sequences form distinct domains such that each can function independently without interfering with the other's functionality, a fact that is also consistent with the ability of the fused protein to show fluorescence.

Because all *mtacp* single and double mutants were viable, we tested whether combining mutations at all three *mtACP* loci was also viable. We genotyped 98 progeny obtained from selfing plants that are heterozygous mutants at all three mtACP genes (i.e. parents with the genotype *mtACP1/mtacp1 mtACP2/mtacp2 mtACP3/mtacp3*), expecting that 1:64 of the seedlings would be homozygous triple mutants. We were unable to find a homozygous triple mutant despite the fact that we readily recovered plants that were homozygous mutant at two *mtACP* loci and heterozygous at the third. Specifically, we were able to recover plants with the following three genotypes: (1) *mtacp1/mtacp1 mtacp2/mtacp2 mtACP3/mtacp3*; (2) *mtacp1/mtacp1 mtACP2/mtacp2 mtacp3/mtacp3*; and (3) *mtACP1/mtacp1 mtacp2/mtacp2 mtacp3/mtacp3*.

Of these three recovered genotypes, only the *mtacp1/mtacp1 mtacp2/mtacp2 mtACP3/mtacp3* mutant revealed a slow growth phenotype that is similar to the *mtacp1 mtacp2* double mutant, and all other recovered genotypes showed no observable growth defects (Supplemental Fig. S6). That only one wild-type allele of *mtACP1* or *mtACP2* is able to support the normal growth of these plants reinforces the conclusion that these two genes are functionally more significant in supporting plant growth and development than is *mtACP3*.

Moreover, the germplasm resulting from selfing each of the above lines enabled more direct evaluation of the effect of the absence of mtACP (Fig. 5). Because the

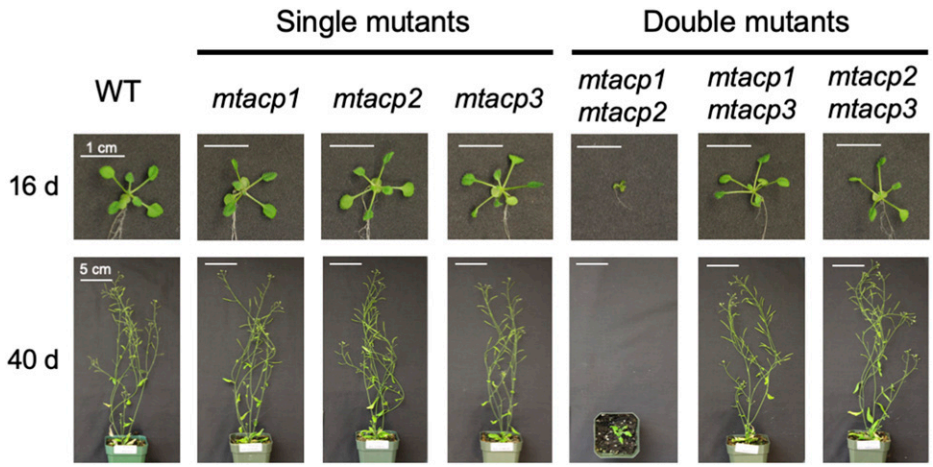

Figure 4. Morphological phenotypes of *mtacp* single and double mutants. Images were taken of plants at 16 d and 40 d post imbibition. WT, Wild type.

mtacp1/mtacp1 mtacp2/mtacp2 mtACP3/mtacp3 mutation caused a growth delay and generated fewer seeds, we focused these experiments on following the segregation ratio in the progeny families generated by selfing either *mtacp1/mtacp1 mtACP2/mtacp2 mtacp3/mtacp3* or *mtACP1/mtacp1 mtacp2/mtacp2 mtacp3/mtacp3* parents, which did not suffer any growth defects. In the siliques of these plants, ~25% seeds were aborted during development, which is consistent with the expected 3:1 Mendelian segregation ratio for a recessive essential gene (*P*-values of the χ^2 tests are 0.93 and 0.6, respectively). Genotyping the progeny from these parents established that out of 240 plants, no homozygous triple mutants were recovered. Taken together, therefore, we deduce from these findings that the homozygous triple mutant, which would lack any mtACP protein, is embryo-lethal, indicating the essential role of mtACP during plant embryogenesis. This is consistent with the embryo-lethal phenotype that is associated with the *mtppt* mutation that is incapable of activating the *apo*-mtACP isoform (Guan et al., 2015).

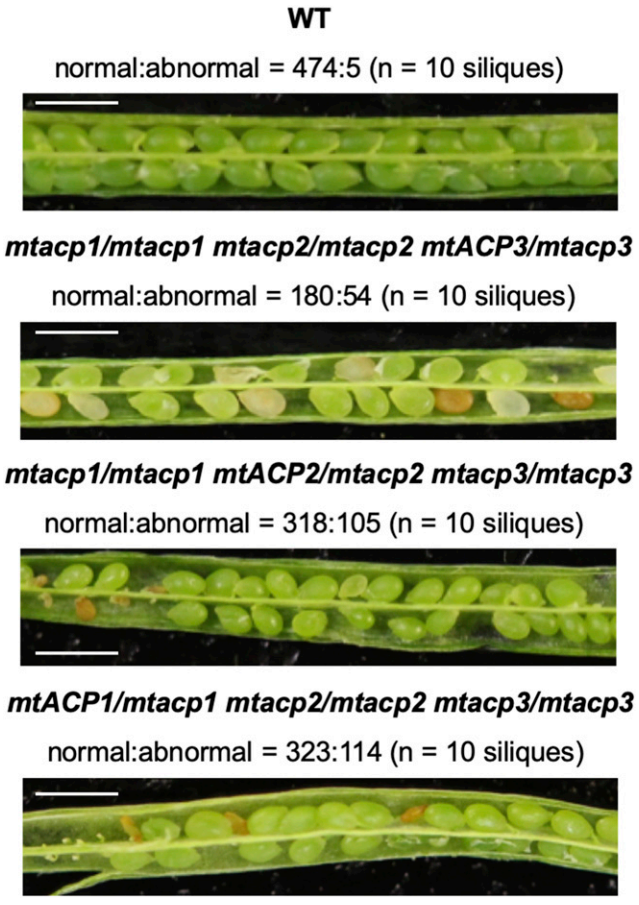

Figure 5. Seed development phenotypes of *mtacp* mutants. Images of siliques developing on selfed progeny of the indicated genotypes. One side of the ovary wall was removed from the fully elongated, fresh silique to reveal the developing seeds. The abnormal seeds are brown or white. Scale bars = 1 mm. WT, Wild type.

Altered Protein Lipoylation Status in the *mtacp1 mtacp2* Mutant

Because of the embryo-lethal phenotype associated with the homozygous triple mutant, we used the *mtacp1 mtacp2* double mutant, which is viable but suffers a growth defect, to examine the physiological roles of mtACPs after embryogenesis. Prior characterizations have indicated that the mtFAS system provides the fatty acid precursor for lipoic acid biosynthesis (Ewald et al., 2007). Therefore, we evaluated the protein lipoylation status of the H subunit of Gly decarboxylase (GDC) in the *mtacp1 mtacp2* mutant lines. SDS-PAGE analysis of these extracts indicated that the expressed proteomes of the *mtacp1 mtacp2* double mutant plants were indistinguishable from the wild-type controls (Fig. 6A). Moreover, immunoblot analysis with anti-H protein antibodies revealed that its accumulation was unchanged from the wild-type levels (Fig. 6B). However, the parallel analysis of the identical extracts with antilipoic acid antibodies revealed that the lipoylation status of this protein was reduced dramatically in the *mtacp1 mtacp2* mutant lines (Fig. 6B). Additionally, these latter analyses revealed that the lipoylated forms of the E2 subunits of mitochondrial pyruvate dehydrogenase (PDH) and α-ketoglutarate dehydrogenase (KGDH) were also reduced to 10% and 35%, respectively, of the wild-type levels in these double mutant plants (Fig. 6B). Additional immunological or mass-spectrometric analyses could assess whether or not accumulation of the latter two proteins is affected in the double mutant; a lack of effect would confirm that the lipoylation status of the E2 subunits of PDH and KGDH is also reduced in the *mtacp1 mtacp2* double mutant lines. Hence, these results link the role of mtACPs with the mtFAS system that contributes to the generation of the lipoic acid cofactor needed for GDC functionality and possibly the other two lipoylated mitochondrial enzymes (i.e. PDH and KGDH).

Altered Metabolome in the *mtacp1 mtacp2* Mutant

More detailed insights into the growth phenotype of the *mtacp1 mtacp2* double mutant were gained by metabolomic profiling. Using GC-MS, we compared the metabolome of 16-d-old double mutant and wild-type seedlings grown in ambient air. In total, 59 metabolites were identified and quantified, and these metabolites were classified as amino acids and amines, sugars, organic acids, and lipids. In the double mutant seedlings, there were statistically significant differences in the levels of 43 metabolites compared to wild-type levels (Fig. 7A). The most drastic change was a 5-fold increase of Gly (Supplemental Dataset S2), which mirrors the alteration in the lipoylation status of the H subunit of GDC (Fig. 6B) that contributes to the catabolism of photorespiratory-derived Gly. Seven additional amino acids (i.e. Val, Ser, Pro, Asn, Ala, Gln, and Orn) exhibited a 2- to 4-fold increase in accumulation.

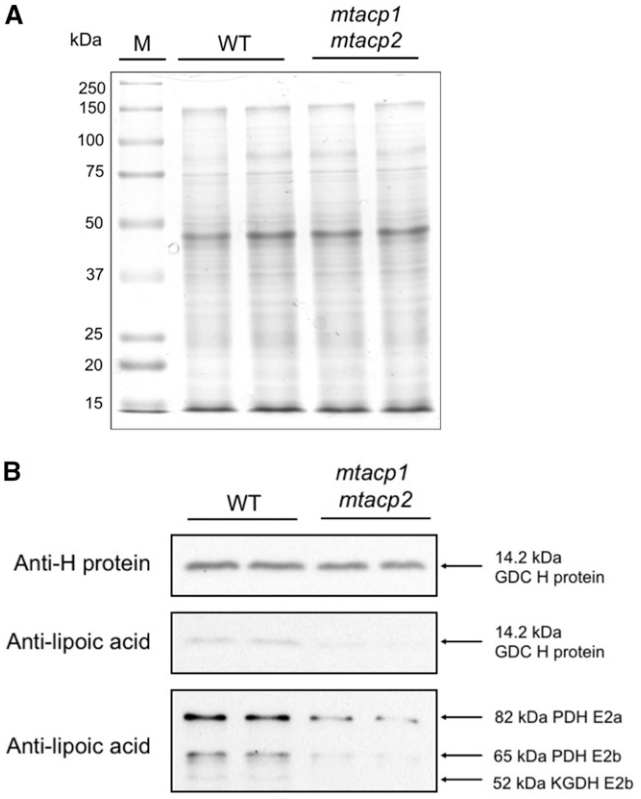

Figure 6. Protein lipoylation status in *mtacp1 mtacp2* double mutant plants. A, Coomassie Brilliant Blue-stained SDS-PAGE analysis of protein extracts prepared from leaves of the indicated genotypes. M, Protein molecular weight markers; WT, wild type. B, Immunoblot analysis using antilipoic acid antibody to identify the lipoylation status of the H subunit of GDC, the E2a and E2b subunits of PDH, and the E2b subunit of KGDH. The accumulation of the H protein subunit was determined in parallel using anti H-protein antibodies.

In contrast, accumulation of another 35 metabolites was decreased to between 20% and 75% of wild-type levels; these included amino acids (i.e. Asp and Glu), sugars (i.e. Glc, Fru, and Suc), organic acids (i.e. fumarate and glycerate), and fatty acids (i.e. 16:1, 16:2, 22:0, 24:0, 26:0, 28:0, and 3-hydroxy 16:0; Supplemental Dataset S2).

Environmental Complementation of the *mtacp1 mtacp2* Mutant

The inhibition of growth and development associated with the *mtacp1 mtacp2* double mutant plants can be partially reversed when these plants are grown in an atmosphere containing 1% CO_2, a condition that inhibits photorespiration. Specifically, as compared to growth in ambient atmospheric conditions, these growth conditions induced the development of two additional rosette leaves by 16 d after imbibition (Fig. 7B). In parallel, the measured metabolome of these plants became more like that of the wild-type (Fig. 7A), with a decrease in the hyperaccumulation of photorespiratory-derived Gly levels (Supplemental Dataset S2). These data are consistent with the role of mtACP in supporting mtFAS to generate the lipoic acid needed to metabolically dispense with photorespiratory-derived intermediates. Additional data that support this conclusion were obtained by growing these double mutant plants in an ambient atmosphere but in the presence of 2% Suc, which supplemented the loss of fixed carbon associated with the inability to recover photorespired carbon due to the block at the GDC-catalyzed reaction. Thus, in these Suc-supplemented plants, the levels of 80% of the metabolites that were altered by the double *mtacp1 mtacp2* mutation were returned to near wild-type levels (Fig. 7A; Supplemental Dataset S2).

DISCUSSION

ACP serves as a metabolic shuttle, iteratively delivering the growing acyl chain intermediates between each enzymatic component of the FAS machinery. In the Type I FAS system, which is primarily present in the cytosol of animal and yeast cells, ACP exists as a domain within a multidomain enzyme that integrates all catalytic components needed for fatty acid biosynthesis (Leibundgut et al., 2008). In the Type II FAS system, which is the predominant fatty acid-generating system in bacteria and plants (White et al., 2005) and is also found in the mitochondria of animal and yeast cells (Hiltunen et al., 2009), a discrete soluble ACP is used to tether the fatty acyl intermediates to the phosphopantetheine cofactor as they are shuttled among individual monofunctional enzymes for fatty acid biosynthesis (White et al., 2005). Plant cells harbor two distinct Type II FAS systems for the de novo biosynthesis of fatty acids, one located in plastids and the other in mitochondria (Ohlrogge and Browse, 1995; Wada et al., 1997). Thus, this twin subcellular compartmentation of the FAS systems requires two sets of constituent enzymes and cofactors in each compartment. While most of the enzymatic components in both FAS systems are encoded by a single gene, eight ACP isoforms are found in the genome of Arabidopsis, of which five are plastidic and three appear to be mitochondrial (Mekhedov et al., 2000). In this study, we experimentally demonstrate the mitochondrial localization of three mtACPs by transgenic expression of *mtACP1*, *mtACP2*, or *mtACP3* genes fused to the GFP-reporter.

The high degree of redundancy of ACPs poses a challenge for functional analysis of each individual ACP. Although several studies have revealed the tissue-specific expression patterns of ptACPs and their impacts on fatty acid composition and adaptation to environmental stimulus (Hloušek-Radojčić et al., 1992; Bonaventure and Ohlrogge, 2002; Ajjawi et al., 2010; Huang et al., 2017), the physiological relevance of the mtACP isoforms remains poorly understood.

Recent characterizations of the mtFAS components have suggested the important role of mtFAS in plant

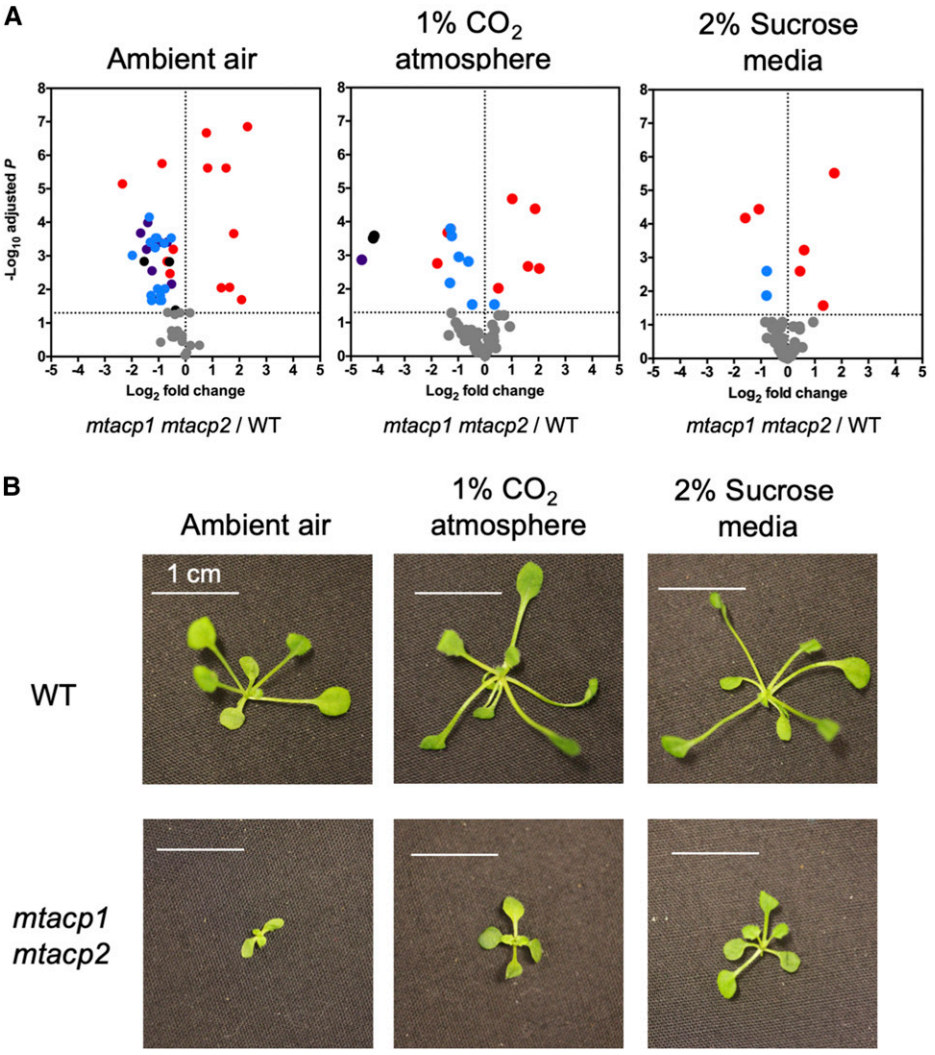

Figure 7. Morphological and metabolic phenotypes of the *mtacp1 mtacp2* double mutant at 16 d postimbibition. A, Alterations in the metabolome of the whole seedlings of the *mtacp1 mtacp2* double mutant as compared to the wild-type (WT) seedlings grown in either an ambient atmosphere, an atmosphere containing 1% CO_2, or on media containing 2% Suc. The *x* axes represent the fold change (on a log-base 2 scale) of the relative abundance of each metabolite in the double mutant versus the wild-type plants. The colored data points above the horizontal dashed gray line indicate statistically significant changes in metabolite levels ($P < 0.05$, $n = 5$; false discovery rate-adjusted Student's *t* test). The data points in each plot represent 59 metabolites that were chemically identified (listed in Supplemental Dataset S2); these include amino acids (red data points), organic acids (purple data points), sugars (black data points), and lipids (blue data points). B, Morphological phenotypes of wild-type and mutant seedlings grown in ambient air, 1% CO_2 atmosphere, or 2% Suc-containing media.

growth and development, particularly as related to lipoic acid biosynthesis (Ewald et al., 2007; Guan and Nikolau, 2016; Guan et al., 2017). In this study, we focus on addressing the in planta function(s) of the three mtACP isoforms. Here, we provide a comprehensive assessment of the functional redundancy and physiological importance of the three mtACPs by systematic mutant analysis and metabolomic analysis.

Redundant mtACP Isoforms Are Essential for Embryogenesis

Genetic analysis established that eliminating the expression of all three *mtACPs* is not viable, indicating the essential role of mtFAS in embryogenesis. In line with this finding, mutation in the gene encoding mtPPT, which activates *apo*-mtACPs by phosphopantetheinylation, leads to an embryo-lethal phenotype (Guan et al., 2015). Thus, the lethality caused by eliminating the expression of all three mtACPs or mtPPT indicates that all three *apo*-mtACP isoforms are substrates of mtPPT, and that active mtACPs support a key process required for embryogenesis.

Prior biochemical analyses indicate that mtPPT is only capable of phosphopantetheinylating the mature *apo*-mtACP isoforms without the mitochondrial targeting sequence (Guan et al., 2015). Collectively, these findings imply that the *holo*-mtACP is first imported into mitochondria before the posttranslational phosphopantetheinylation of the specific target Ser residue. This contrasts with the phosphopantetheinylation mechanism of mammalian mtACP, which is activated by a cytosolic PPT prior to import into mitochondria (Joshi et al., 2003).

The viability of *mtacp* single and double mutants suggests functional redundancy among the three mtACP isoforms. The degree of this redundancy is correlated to the relative expression levels of each isoform. For example, plants that express only *mtACP3* suffer a drastic delay in growth and show dramatic morphological developmental aberrations. This contrasts with the normal morphology and growth of the other two double mutant combinations, which singularly

express either mtACP1 or mtACP2, and with that of all single mutants. Thus, the low expression of *mtACP3* is probably the reason it cannot solely compensate for the loss of *mtACP1* and *mtACP2*, whereas the much higher expression levels of either of the latter two genes is sufficient to compensate for the missing *mtACP1* and *mtACP3* or *mtACP2* and *mtACP3* genes in the relevant double mutants. We conclude, therefore, that *mtACP1* and *mtACP2* have a more prominent role in supporting mtFAS than does *mtACP3*.

Such complex and unequal functional redundancy among mtACP isoforms does not occur in other organisms. For example, only one mtACP isoform is expressed in the mitochondria of yeast and human cells (Brody et al., 1997; Feng et al., 2009). In the genome of *C. reinhardtii*, a green microalga, two ACP isoforms have been identified, one associated with plastids and the other with mitochondria (Blatti et al., 2012). Our phylogenetic analysis revealed the conservation of three mtACP isoforms in monocot and dicot species, suggesting that the development of multiple ACP isoforms is an attribute associated with Plantae, and this appears to have occurred during early stages of plant evolution.

mtACP Contribution to mtFAS Supports the Recovery of Photorespired Carbon

Because mtACP is an essential component of Type II FAS systems, mutants that lack mtACP expression provide insights into the physiological role of mtFAS. Thus, the characterization of the viable, but growth-affected, *mtacp1 mtacp2* double mutant provides insights concerning this physiological function. Consistent with earlier biochemical studies that indicated the role of mtFAS in generating the octanoate precursor of lipoic acid biosynthesis (Wada et al., 1997), this double mutant shows depleted lipoylation of mitochondrial GDC. A direct metabolic consequence of under-lipoylation of mitochondrial GDC is the accumulation of Gly, which was observed when *mtacp1 mtacp2* double mutant plants were grown in ambient air. Moreover, when these plants are grown in an elevated CO_2 atmosphere, which reduces photorespiratory flux by suppressing the oxygenation reaction of Rubisco, the hyperaccumulation of Gly is reduced to wild-type levels. These metabolic alterations resemble those previously observed with other mtFAS mutants (Guan et al., 2015, 2017). Therefore, the involvement of mtACP in the mtFAS system in supporting lipoic acid biosynthesis appears to be conserved in plants, yeast, and humans (Wada et al., 1997; Hiltunen et al., 2010). In addition, accumulation of 3-hydroxyhexadecanoic acid is reduced in the *mtacp1 mtacp2* double mutant. This fatty acid is a component of lipid A, a component of the outer membrane of gram-negative bacteria (Bainbridge et al., 2008). This finding substantiates the role of mtFAS function in generating the precursor for the assembly of lipid A-like molecules in plants (Guan et al., 2017).

Unlike many mtFAS mutants, which express normal growth phenotypes when grown in an elevated CO_2 atmosphere, the extremely stunted phenotype of the *mtacp1 mtacp2* double mutant is only partially rescued by the elevated CO_2 atmosphere. This is further authenticated by the finding that the metabolome of the *mtacp1 mtacp2* double mutant is not completely reversed to the wild-type state when these plants are grown in the elevated CO_2 atmosphere. On the one hand, one cannot exclude the possibility that these metabolic changes may be associated with the decreased lipoylation status of mitochondrial PDH and KGDH, which would generate photorespiration-independent metabolic alterations. On the other hand, the metabolic changes associated with the *mtacp1 mtacp2* double mutant were not observed in previously characterized mtFAS mutants, suggesting that the depletion of mtACPs has a more complex impact on the metabolic processes that are independent of mtFAS function. Thus, it's plausible that these non-mtFAS-associated functions may be the cause of the failed embryogenesis in plants only expressing mtACP3. Previous studies with other eukaryotic organisms have demonstrated that mtACPs are connected to cellular processes that are beyond mitochondrial fatty acid metabolism. For example, in mammalian and yeast cells, mtACP is involved in maintaining the integrity of several mitochondrial complexes, including respiratory complexes and the biosynthesis of Fe-S cluster complexes (Van Vranken et al., 2016; Majmudar et al., 2019). In another example, the acylated form of mtACP1 has been reported to be associated with the mitochondrial membrane of Arabidopsis (Shintani and Ohlrogge, 1994), whereas another study found that this protein is present in the mitochondrial matrix (Meyer et al., 2007).

In summary, we have demonstrated the physiological roles of three mtACP isoforms of mitochondrially localized mtFAS machinery and identified that mtACP1 and mtACP2 are the predominant isoforms that support this metabolic functionality. Our results expand on the role of mtFAS in providing the precursor needed for lipoic acid biosynthesis, and we also present evidence that mtACP isoforms may be involved in other processes that appear to be particularly required during embryogenesis.

MATERIALS AND METHODS

Phylogenetic Analysis

Identification of ACP protein sequences in different plant species was performed by searching the National Center for Biotechnology Information database using Arabidopsis (*Arabidopsis thaliana*) mtACP1 encoded by At2g44620, mtACP2 encoded by At1g65290, mtACP3 encoded by At5g47630, ptACP1 encoded by At3g05020, ptACP2 encoded by At1g54580, ptACP3 encoded by At1g54630, ptACP4 encoded by At4g25050, and ptACP5 encoded by At5g27200 as queries. The accession numbers of the achieved amino acid sequences are listed in Supplemental Dataset S1. The phylogenetic tree of plant ACP homologs was constructed using the neighbor-joining method in MEGAX (Kumar et al., 2018) and visualized using iTOL (Letunic and Bork, 2016).

A bootstrapping method with 1,000 replicates was used to test the reliability of the tree.

Plant Materials and Genetic Transformations

Seed stocks of the Arabidopsis T-DNA insertional mutant lines were obtained from the Arabidopsis Biological Resource Center (http://abrc.osu.edu/): SAIL_912_B05 for *mtACP1*, SALK_073185 for *mtACP2*, and SALK_127678 for *mtACP3*. All mutant alleles are in the same wild-type background (ecotype Columbia of Arabidopsis [Col-0]). Homozygous *mtacp1*, *mtacp2*, and *mtacp3* mutant alleles were identified by PCR-genotyping. The precise T-DNA insertion positions in each allele of the *mtACP* genes were verified by sequencing (Supplemental Fig. S3). The double mutant and triple mutant stocks were generated by crosses between three single mutant alleles.

For the GFP experiments, the ORF encoding *mtACP1*, *mtACP2*, and *mtACP3* was cloned into the pENTR/D-TOPO vector (Invitrogen) and subcloned into pEarleyGate103 (Earley et al., 2006) using Gateway LR Clonase II Enzyme Mix (Invitrogen). The resulting vectors carrying the *p35S::mtACP1-GFP*, *p35S::mtACP2-GFP*, and *p35S::mtACP3-GFP* were used to transform Arabidopsis Col-0 wild-type plants as previously described (Clough and Bent, 1998). For the genetic complementation experiment, *p35S::mtACP2-GFP* was used to transform the *mtacp1 mtacp2* double mutant plants. Primer sequences used for cloning are listed in Supplemental Table S2.

For plate-grown plants, seeds were sterilized and placed on one-half strength Murashige and Skoog (MS) growth medium supplemented with a vitamin mixture (Sigma-Aldrich). In the Suc feeding experiments, the agar medium was supplemented with 2% (w/v) Suc and was adjusted to pH 5.7 with 0.1 N KOH before adding 1.5% (w/v) agar. Seeds were stratified for 2 d at 4°C in the dark and transferred to a continuously illuminated growth chamber (100 μmol m^{-2} s^{-1}) at 22°C and 60% relative humidity. The plates were transferred to growth chambers flushed with ambient air or 1% (v/v) CO_2. For soil-grown plants, seedlings were grown on plates for 10 d before being transferred into potting mix.

Confocal Microscopy Analysis

Confocal microscopy was conducted on wild-type control plants and the T3 generation of transgenic plants expressing the GFP-tagged proteins. Root tissues from 7-d-old seedling plants were randomly collected and stained with 200 nM MitoTracker Orange (Invitrogen) for 15 min as described previously (Guan et al., 2015). After staining, roots were washed in one-half strength MS solution for 15 min and visualized with a Leica SP5 X confocal microscope system (Leica Microsystems; http://www.leica-microsystems.com/). The laser wavelengths were set as follows: an emission band of 500 to 535 nm for GFP (excitation 489 nm) and an emission band of 560 to 600 nm for MitoTracker Orange (excitation 543 nm).

RNA Extraction and RT-qPCR Analysis

Total RNA was extracted from 100 mg of different Arabidopsis tissues using TriZol (Invitrogen) according to the manufacturer's instructions. Contaminating DNA was removed by using a TURBO DNA-free kit (Invitrogen). RNA concentration was determined with a NanoDrop ND1000 Spectrophotometer (Thermo Fisher Scientific). Complementary DNA synthesis was performed using the complementary DNA EcoDry Premix-Double Primed Kit (Clontech) using 5 μg of RNA as the template. RT-qPCR was performed using the StepOnePlus detection system (Applied Biosystems) and PowerUp SYBR Green Master Mix (Applied Biosystems). *Ubiqutin 10* (*UBQ10*, At4g05320) was used as the reference gene for relative quantification. Primer sequences are listed in Supplemental Table S2.

Protein Extraction and Immunoblotting

Total protein was extracted from 0.1 g of leaves from 16-d-old seedlings as described previously (Che et al., 2002). The extracted proteins were separated on 12.5% SDS-PAGE, then transferred onto nitrocellulose membranes. Immunoblot analysis was performed with antilipoic acid antibodies or with anti-H protein antibodies, as described previously (Ewald et al., 2007; Guan et al., 2017).

Metabolomic Profiling

Polar metabolites were extracted from 3 mg of lyophilized tissues and trimethylsilyl (TMS) derivatized as described previously (McVey et al., 2018). Fatty acids were extracted and transmethylated from 3 mg of dry tissues as described previously (Lu et al., 2008). The derivatized samples were analyzed using an Agilent 7890 GC-MS system equipped with Agilent HP-5 ms column. The peak area of each metabolite was normalized to the peak area of an internal standard (nor-Leu for polar metabolites and nonadecanoic acid for fatty acids) and sample dry weight. The means of five or six biological replicates were used to determine the fold changes between the mutant line and the wild type. A false discovery rate-adjusted Student's *t* test (Benjamini and Hochberg, 1995) was used to identify metabolites that were significantly changed in the mutant relative to the wild type.

Accession Numbers

Sequence data from this article can be found in the GenBank/EMBL data libraries under the following accession numbers: At2g44620 (*mtACP1*, gene identifier (ID) 819070); At1g65290 (*mtACP2*, gene ID 842836); and At5g47630 (*mtACP3*, gene ID 834813).

Supplemental Data

The following supplemental materials are available.

Supplemental Figure S1. Comparison of the amino acid sequences of the eight ACP isoforms encoded by the Arabidopsis genome.

Supplemental Figure S2. Relative expression levels of the *mtACP* mRNAs at different developmental stages.

Supplemental Figure S3. Characterization of *mtacp1*, *mtacp2*, and *mtacp3* T-DNA-tagged alleles.

Supplemental Figure S4. Plant biomass produced by *mtacp* single and double mutant seedlings at 16 d post imbibition.

Supplemental Figure S5. Transgenic complementation of the *mtacp1 mtacp2* homozygous double mutant by expression of the *p35S::mtACP2-GFP* transgene.

Supplemental Figure S6. Morphological phenotypes of *mtacp* mutants, homozygous at two *mtACP* loci and heterozygous at the third.

Supplemental Table S1. In silico predictions of the subcellular localization of mtACP1, mtACP2, and mtACP3.

Supplemental Table S2. Sequences of the DNA primers used in this study.

Supplemental Dataset S1. List of accession numbers of ACP homologs used to generate the phylogenetic tree shown in Figure 1.

Supplemental Dataset S2. Metabolite profiling revealed differential metabolic changes of the *mtacp1 mtacp2* double mutant seedlings under different conditions.

ACKNOWLEDGMENTS

The authors acknowledge Dr. Ann Perera, Dr. Lucas Showman, and Dr. Zhihong Song of the WM Keck Metabolomics Research Laboratory (Iowa State University) for providing guidance in the metabolite profiling experiments; the Roy J. Carver High Resolution Microscopy Facility (Iowa State University) for providing access to confocal microscopy; and Febriana Pangestu, Hannah Yang, and Rahne McIntire (Iowa State University) for assisting in screening plant mutants.

Received November 27, 2019; accepted February 10, 2020; published February 24, 2020.

LITERATURE CITED

Ajjawi I, Lu Y, Savage LJ, Bell SM, Last RL (2010) Large-scale reverse genetics in Arabidopsis: Case studies from the Chloroplast 2010 Project. Plant Physiol **152:** 529–540

Bainbridge BW, Karimi-Naser L, Reife R, Blethen F, Ernst RK, Darveau RP (2008) Acyl chain specificity of the acyltransferases LpxA and LpxD and substrate availability contribute to lipid A fatty acid heterogeneity in *Porphyromonas gingivalis*. J Bacteriol **190:** 4549–4558

Benjamini Y, Hochberg Y (1995) Controlling the false discovery rate: A practical and powerful approach to multiple testing. J R Stat Soc Series B Stat Methodol **57:** 289–300

Blatti JL, Beld J, Behnke CA, Mendez M, Mayfield SP, Burkart MD (2012) Manipulating fatty acid biosynthesis in microalgae for biofuel through protein-protein interactions. PLoS One **7:** e42949

Bonaventure G, Ohlrogge JB (2002) Differential regulation of mRNA levels of acyl carrier protein isoforms in Arabidopsis. Plant Physiol **128:** 223–235

Branen JK, Shintani DK, Engeseth NJ (2003) Expression of antisense acyl carrier protein-4 reduces lipid content in Arabidopsis leaf tissue. Plant Physiol **132:** 748–756

Brody S, Oh C, Hoja U, Schweizer E (1997) Mitochondrial acyl carrier protein is involved in lipoic acid synthesis in *Saccharomyces cerevisiae*. FEBS Lett **408:** 217–220

Che P, Wurtele ES, Nikolau BJ (2002) Metabolic and environmental regulation of 3-methylcrotonyl-coenzyme A carboxylase expression in Arabidopsis. Plant Physiol **129:** 625–637

Chuman L, Brody S (1989) Acyl carrier protein is present in the mitochondria of plants and eucaryotic micro-organisms. Eur J Biochem **184:** 643–649

Clough SJ, Bent AF (1998) Floral dip: A simplified method for *Agrobacterium*-mediated transformation of *Arabidopsis thaliana*. Plant J **16:** 735–743

Earley KW, Haag JR, Pontes O, Opper K, Juehne T, Song K, Pikaard CS (2006) Gateway-compatible vectors for plant functional genomics and proteomics. Plant J **45:** 616–629

Ewald R, Kolukisaoglu U, Bauwe U, Mikkat S, Bauwe H (2007) Mitochondrial protein lipoylation does not exclusively depend on the mtKAS pathway of de novo fatty acid synthesis in Arabidopsis. Plant Physiol **145:** 41–48

Feng D, Witkowski A, Smith S (2009) Down-regulation of mitochondrial acyl carrier protein in mammalian cells compromises protein lipoylation and respiratory complex I and results in cell death. J Biol Chem **284:** 11436–11445

Guan X, Chen H, Abramson A, Man H, Wu J, Yu O, Nikolau BJ (2015) A phosphopantetheinyl transferase that is essential for mitochondrial fatty acid biosynthesis. Plant J **84:** 718–732

Guan X, Nikolau BJ (2016) AAE13 encodes a dual-localized malonyl-CoA synthetase that is crucial for mitochondrial fatty acid biosynthesis. Plant J **85:** 581–593

Guan X, Okazaki Y, Lithio A, Li L, Zhao X, Jin H, Nettleton D, Saito K, Nikolau BJ (2017) Discovery and characterization of the 3-hydroxyacyl-ACP dehydratase component of the plant mitochondrial fatty acid synthase system. Plant Physiol **173:** 2010–2028

Guerra DJ, Ohlrogge JB, Frentzen M (1986) Activity of acyl carrier protein isoforms in reactions of plant fatty acid metabolism. Plant Physiol **82:** 448–453

Hiltunen JK, Schonauer MS, Autio KJ, Mittelmeier TM, Kastaniotis AJ, Dieckmann CL (2009) Mitochondrial fatty acid synthesis type II: More than just fatty acids. J Biol Chem **284:** 9011–9015

Hiltunen JK, Chen Z, Haapalainen AM, Wierenga RK, Kastaniotis AJ (2010) Mitochondrial fatty acid synthesis—An adopted set of enzymes making a pathway of major importance for the cellular metabolism. Prog Lipid Res **49:** 27–45

Hloušek-Radojčić A, Post-Beittenmiller D, Ohlrogge JB (1992) Expression of constitutive and tissue-specific acyl carrier protein isoforms in Arabidopsis. Plant Physiol **98:** 206–214

Hruz T, Laule O, Szabo G, Wessendorp F, Bleuler S, Oertle L, Widmayer P, Gruissem W, Zimmermann P (2008) Genevestigator v3: A reference expression database for the meta-analysis of transcriptomes. Adv Bioinforma **2008:** 420747

Huang J, Xue C, Wang H, Wang L, Schmidt W, Shen R, Lan P (2017) Genes of ACYL CARRIER PROTEIN family show different expression profiles and overexpression of ACYL CARRIR PROTEIN 5 modulates fatty acid composition and enhances salt stress tolerance in *Arabidopsis*. Front Plant Sci **8:** 987

Joshi AK, Zhang L, Rangan VS, Smith S (2003) Cloning, expression, and characterization of a human 4′-phosphopantetheinyl transferase with broad substrate specificity. J Biol Chem **278:** 33142–33149

Kumar S, Stecher G, Li M, Knyaz C, Tamura K (2018) MEGA X: Molecular evolutionary genetics analysis across computing platforms. Mol Biol Evol **35:** 1547–1549

Lambalot RH, Gehring AM, Flugel RS, Zuber P, LaCelle M, Marahiel MA, Reid R, Khosla C, Walsh CT (1996) A new enzyme superfamily—The phosphopantetheinyl transferases. Chem Biol **3:** 923–936

Leibundgut M, Maier T, Jenni S, Ban N (2008) The multienzyme architecture of eukaryotic fatty acid synthases. Curr Opin Struct Biol **18:** 714–725

Letunic I, Bork P (2016) Interactive tree of life (iTOL) v3: An online tool for the display and annotation of phylogenetic and other trees. Nucleic Acids Res **44**(W1): W242–W245

Lu Y, Savage LJ, Ajjawi I, Imre KM, Yoder DW, Benning C, Dellapenna D, Ohlrogge JB, Osteryoung KW, Weber AP, et al (2008) New connections across pathways and cellular processes: Industrialized mutant screening reveals novel associations between diverse phenotypes in Arabidopsis. Plant Physiol **146:** 1482–1500

Majmudar JD, Feng X, Fox NG, Nabhan JF, Towle T, Ma T, Gooch R, Bulawa C, Yue WW, Martelli A (2019) 4′-Phosphopantetheine and long acyl chain-dependent interactions are integral to human mitochondrial acyl carrier protein function. MedChemComm **10:** 209–220

Markham JE, Molino D, Gissot L, Bellec Y, Hématy K, Marion J, Belcram K, Palauqui J-C, Satiat-Jeunemaître B, Faure JD (2011) Sphingolipids containing very-long-chain fatty acids define a secretory pathway for specific polar plasma membrane protein targeting in *Arabidopsis*. Plant Cell **23:** 2362–2378

McVey PA, Alexander LE, Fu X, Xie B, Galayda K-J, Nikolau BJ, Houk RS (2018) Light-dependent changes in the spatial localization of metabolites in *Solenostemon scutellarioides* (coleus Henna) visualized by matrix-free atmospheric pressure electrospray laser desorption ionization mass spectrometry imaging. Front Plant Sci **9:** 1348

Mekhedov S, de Ilárduya OM, Ohlrogge J (2000) Toward a functional catalog of the plant genome. A survey of genes for lipid biosynthesis. Plant Physiol **122:** 389–402

Meyer EH, Heazlewood JL, Millar AH (2007) Mitochondrial acyl carrier proteins in *Arabidopsis thaliana* are predominantly soluble matrix proteins and none can be confirmed as subunits of respiratory Complex I. Plant Mol Biol **64:** 319–327

Ohlrogge JB, Kuo TM (1985) Plants have isoforms for acyl carrier protein that are expressed differently in different tissues. J Biol Chem **260:** 8032–8037

Ohlrogge J, Browse J (1995) Lipid biosynthesis. Plant Cell **7:** 957–970

Samuels L, Kunst L, Jetter R (2008) Sealing plant surfaces: Cuticular wax formation by epidermal cells. Annu Rev Plant Biol **59:** 683–707

Shintani DK, Ohlrogge JB (1994) The characterization of a mitochondrial acyl carrier protein isoform isolated from *Arabidopsis thaliana*. Plant Physiol **104:** 1221–1229

Simoni RD, Criddle RS, Stumpf PK (1967) Fat metabolism in higher plants. XXXI. Purification and properties of plant and bacterial acyl carrier proteins. J Biol Chem **242:** 573–581

The Angiosperm Phylogeny Group (2016) An update of the Angiosperm Phylogeny Group classification for the orders and families of flowering plants: APG IV. Bot J Linn Soc **181:** 1–20

Van Vranken JG, Jeong M-Y, Wei P, Chen Y-C, Gygi SP, Winge DR, Rutter J (2016) The mitochondrial acyl carrier protein (ACP) coordinates mitochondrial fatty acid synthesis with iron sulfur cluster biogenesis. eLife **5:** e17828

Wada H, Shintani D, Ohlrogge J (1997) Why do mitochondria synthesize fatty acids? Evidence for involvement in lipoic acid production. Proc Natl Acad Sci USA **94:** 1591–1596

White SW, Zheng J, Zhang Y-M, Rock CO (2005) The structural biology of type II fatty acid biosynthesis. Annu Rev Biochem **74:** 791–831